Effect of Metal Ions and Adenylylation State on the Internal Thermodynamics of Phosphoryl Transfer in the *Escherichia coli* Glutamine Synthetase Reaction†

Lynn M. Abell and Joseph J. Villafranca*
Department of Chemistry, The Pennsylvania State University, University Park, Pennsylvania 16802
Received July 10, 1990; Revised Manuscript Received October 22, 1990

ABSTRACT: Experiments were conducted to study the differences in catalytic behavior of various forms of *Escherichia coli* glutamine synthetase. The enzyme catalyzes the ATP-dependent formation of glutamine from glutamate and ammonia via a γ-glutamyl phosphate intemediate. The physiologically important metal ion for catalysis is Mg^{2+}; however, Mn^{2+} supports in vitro activity, though at a reduced level. Additionally, the enzyme is regulated by a covalent adenylylation modification, and the metal ion specificity of the reaction depends on the adenylylation state of the enzyme. The kinetic investigations reported herein demonstrate differences in binding and catalytic behavior of the various forms of glutamine synthetase. Rapid quench kinetic experiments on the unadenylylated enzyme with either Mg^{2+} or Mn^{2+} as the activating metal revealed that product release is the rate-limiting step. However, in the case of the adenylylated enzyme, phosphoryl transfer is the rate-limiting step. The internal equilibrium constant for phosphoryl transfer is 2 and 5 for the unadenylylated enzyme with Mg^{2+} or Mn^{2+}, respectively. For the Mn^{2+}-activated adenylylated enzyme the internal equilibrium constant is 0.1, indicating that phosphoryl transfer is less energetically favorable for this form of the enzyme. The factors that make the unadenylylated enzyme most active with Mg^{2+} are discussed.

Glutamine synthetase (GS)[1] from *Escherichia coli* requires two divalent metal ions per active site in order to catalyze the ATP-dependent formation of glutamine from glutamate and ammonia. The enzyme plays a central role in ammonia metabolism in both prokaryotic and eukaryotic systems.

$$\text{glutamate} + \text{ATP} + \text{NH}_3 \xrightleftharpoons{2M^{2+}} \text{glutamine} + \text{ADP} + \text{P}_i \quad (1)$$

The enzyme has a molecular weight of 600 000 and is composed of 12 identical subunits arranged in two hexameric rings which are stacked on top of each other. The X-ray crystal structure indicates that the active site is located at the interface of two adjacent subunits in a given hexameric ring (Almassy et al., 1986; Yamashita et al., 1989).

Glutamine synthetase activity in *E. coli* is highly regulated by a number of feedback inhibitors, by a covalent adenylylation modification, and at the level of transcription by the amount of ammonia and other nitrogen sources in the growth media (Stadtman & Ginsburg, 1974). The adenylylation reaction is catalyzed by the enzyme adenyltransferase which transfers the AMP moiety of ATP to tyrosine 397. The adenylylation modification is reversible and is in turn controlled by a closed bicyclic cascade system which is sensitive to the ratio of glutamine and α-ketoglutarate in the cell (Ginsburg & Stadtman, 1973; Stadtman et al., 1980; Magasanik & Reitzer, 1987). The effect of adenylylation on a given subunit is to change the divalent metal ion requirement and the pH for optimal activity (Ginsburg et al., 1970). Unadenylylated subunits show maximal activity with Mg^{2+} at pH 7.5 which is most likely the physiologically important metal ion. Adenylylated subunits on the other hand show maximal activity with Mn^{2+} at pH 6.5.

The chemical mechanism which has been proposed for this enzyme involves the initial formation of a γ-glutamyl phosphate intermediate from ATP and glutamate followed by displacement of the activated phosphate group by ammonia. The catalytic roles proposed for the two divalent metal ions in this reaction are quite different, and they are distinguished from one another by their dissociation constants. The tightly bound n_1 ion is thought to keep the enzyme in its catalytically active conformation. The less tightly bound n_2 metal ion is thought to be involved in nucleotide binding as well as phosphoryl transfer.

The presence of the acid-labile γ-glutamyl phosphate intermediate was previously detected from the observation of a burst of acid-labile phosphate in a rapid quench experiment with low adenylylation state enzyme and Mg^{2+} as the activating metal (Meek et al., 1982). Use of this technique provided not only evidence for the intermediacy of γ-glutamyl phosphate but also offered some insight into the energetics of phosphoryl transfer. Analysis of the burst rate and the slower steady-state rate which followed showed that the internal equilibrium for phosphoryl transfer had a ratio of 1.9 in the forward direction and that product release and not phosphoryl transfer was the rate-limiting step in the reaction pathway.

Despite numerous attempts, no apparent conformational differences between the unadenylylated and adenylylated unliganded enzyme have been detected by ORD (Holzer, 1969), difference sedimentation velocity (Ginsburg, 1972), and protein difference spectral measurements (Ginsburg, 1972; Stadtman & Ginsburg, 1974). However, upon complexation of the enzyme with the tetrahedral transition-state analogue L-methionine (*S*,*R*)-sulfoximine (MSOX), subtle conformational differences between the adenylylated and unadenylylated forms of the enzyme have been observed by UV difference measurements and difference sedimentation velocity studies (Ginsburg, 1972). Calorimetric studies on both the adenyl-

† This work was supported by NIH Grants GM23529 (J.J.V.) and GM11994 (fellowship to L.M.A.).
* To whom correspondence should be addressed.

[1] Abbreviations: GS, glutamine synthetase; $GS_{n=2}$, low adenylylation state enzyme; $GS_{n=12}$, high adenylylation state enzyme; MSOX, L-methionine (*S*,*R*)-sulfoximine; Hepes, *N*-(2-hydroxyethyl)piperazine-*N*′-2-ethanesulfonic acid; PEP, phosphoenolpyruvate; EDTA, ethylenediaminetetraacetic acid; Pipes, 2,2′-piperazine-1,4-diylbis(ethanesulfonic acid).

0006-2960/91/0430-1413$02.50/0

ylated and unadenylylated enzyme in the presence of Mn^{2+} and MSOX have shown that while only a very small change in proton uptake is observed for the unadenylylated enzyme, a net uptake of 1.7 equiv of H^+/mol of subunits or the equivalent protonation of two protein residues accompanies the binding of the analogue to the fully adenylylated enzyme at pH 7.1 (Gorman & Ginsburg, 1982).

The effect of adenylylation and the concommitant structural changes on the chemistry of the glutamine synthetase reaction have not been thoroughly investigated. In order to address this question, rapid quench kinetic techniques were used to determine the effect of metal ion type and adenylylation on the energetics of phosphoryl transfer. Steady-state kinetic measurements were conducted to determine the kinetic properties of both the adenylylated and unadenylylated forms of the enzyme with respect to ATP, glutamate, and both Mg^{2+} and Mn^{2+}. The results of these experiments were then used to design rapid quench experiments in order to study the internal thermodynamics of glutamine synthetase.

Experimental Procedures

Materials. [γ-^{32}P]ATP (10–50 Ci/mmol) was obtained from New England Nuclear and purified prior to use according to Lewis and Villafranca (1989). All other biochemicals were from Sigma and were of the highest purity available.

Enzyme. Glutamine synthetase was purified from *E. coli* YMC10 (Backman et al., 1981). GS is overexpressed in this strain by the plasmid pgln6 which contains *gln*A, the structural gene for glutamine synthetase. Low adenylylation state enzyme ($GS_{n=2}$) was obtained from YMC10/pgln6 grown on minimal media with glucose as the carbon source and glutamine as the sole nitrogen source. In the final growth, $MnCl_2$ was added to a final concentration of 1 mM to inhibit oxidation of GS (Roseman & Levine, 1987). The enzyme was purified according to a variation of the zinc precipitation method (Miller et al., 1974) which included a streptomycin sulfate step, one zinc precipitation step followed by extensive dialysis to remove the zinc, an acetone precipitation step at 0 °C, and a final ammonium sulfate precipitation at pH 4.4 (Rhee et al., 1985).

Adenylylated enzyme ($GS_{n=12}$) was prepared in vitro by using the enzyme adenylyl transferase and the method of Henning and Ginsburg (1971) and then repurified by zinc precipitation and an ammonium sulfate precipitation. After purification, the enzyme was stored at 4 °C in 1 mM $MnCl_2$, 20 mM imidazole, and 100 mM KCl at pH 7.2. While $GS_{n=2}$ retained 100% of its specific activity under these conditions for over a year, the adenylylated enzyme showed a 50% loss in activity after about 6 months.

Protein concentrations were determined by either the BCA assay (Pierce) in the absence of Mn^{2+} or by spectrophotometric methods (Ginsburg et al., 1970). Adenylylation state was determined spectrophotometrically (Shapiro & Stadtman, 1970) and by the transferase assay method (Stadtman et al., 1979).

Low adenylylation state enzyme had an average adenylylation state of 1.4 ± 0.1 and a specific activity of 120 units/mg by transferase assay. $GS_{n=12}$ had an average adenylylation state of 12.1 ± 0.2 and a specific activity of 138 units/mg. Each enzyme was shown to be 95–98% pure by denaturing gel electrophoresis.

The Mn^{2+} form of the enzyme was converted to the Mg^{2+} form by dialysis against several changes of buffer containing EDTA for 12 h and then dialyzed extensively for 36 h against 50 mM Hepes or Pipes, 100 mM KCl, and 25 mM $MgCl_2$ at the desired pH. The specific activity of the enzyme was found to be unchanged after this procedure.

Steady-State Kinetics. The biosynthetic activity at pH 6.5 and 7.5 using either Mg^{2+} or Mn^{2+} as the activating metal ion was monitored spectrophotometrically by coupling ADP production to NADH oxidation using lactate dehydrogenase and pyruvate kinase. The assay mix contained 100 mM Hepes, 100 mM Pipes, 100 mM KCl, 1 mM PEP, 190 μg of NADH, 33 μg/mL pyruvate kinase, and 33 μg/mL L-lactate dehydrogenase. A 5-fold increase in coupling enzymes was required for studies containing Mg^{2+} at pH 6.5. The amount of metal required for optimal activity was determined for each enzyme at a given pH by holding [ATP] and [glutamate] constant and varying the metal ion concentration. When the optimal concentration was determined, a fixed concentration of excess metal ion over ATP was held constant when ATP concentration was varied (Morrison, 1979). The K_m's for ATP and glutamate were determined by varying the concentration of one of the substrates while holding the other fixed at 5–10 times the K_m value. The ammonia concentration was held constant throughout at 50 mM. Assays were performed in 1.0-cm cuvettes with 1.00-mL total volume in a Cary 2200 UV/vis spectrophotometer thermostated at 25 °C. The change in absorbance at 340 nm vs time was monitored. Initial rates of reaction were determined by using SPECTRA CALC.

Stopped-Flow Experiments. Stopped-flow measurements were performed by using an apparatus designed and built at The Pennsylvania State University as described by Johnson (1986). The apparatus has a 1.6-ms dead time, a 2-mm path length, and a thermostated observation cell which was maintained at 25 °C. Enzyme–ATP complex formation was observed by using an excitation wavelength of 300 nm. Emission was observed at 340 nm by using a band-pass filter on the output. An average of four runs was used for data analysis, and a minimum of a 5-fold excess of ATP over enzyme was used to allow pseudo-first-order analysis. Data were collected over 6 half-lives (approximately 20 ms). Rate constants were obtained by fitting the data to a single exponential by an iterative, nonlinear least-squares program using a modification of the method of moments (Johnson, 1986). For experiments with the low adenylylation state enzyme and Mn^{2+}, a 0.1-mL solution containing 10 μM unadenylylated subunits, 100 mM KCl, 8 mM $MnCl_2$, and 50 mM Pipes at pH 6.5 was mixed with an equal volume of solution containing a variable concentration of ATP in the same buffer system. For the adenylylated enzyme, the enzyme concentration was 20 μM in subunits in the same buffer system as the low adenylylation state enzyme with Mn^{2+}. For experiments with the low adenylylation state enzyme with Mg^{2+} as the activating metal, a solution containing 10 μM unadenylylated subunits, 50 mM Hepes, 100 mM KCl, and 25 mM $MgCl_2$ at pH 7.5 was mixed with various concentrations of ATP in identical buffer.

Rapid Quench Experiments. The rapid quench experiments were performed at 10 and 17 °C on an apparatus designed and built by Johnson (1986). The reactions were initiated by the simultaneous mixing of two solutions, one containing enzyme and activating metal ion at the appropriate pH (0.039 mL) and the other containing all substrates (0.042 mL) and trace amounts of [γ-^{32}P]ATP (5000 cpm/nmol of cold ATP). The reactions were quenched with 190 μL of 0.6 N HCl and then immediately neutralized with 45 μL of a solution containing 1 M Tris and 4 N KOH. [γ-^{32}P]P_i was isolated as described by Johnson (1986). All experiments carried out at pH 6.5 contained 100 mM Pipes and 100 mM KCl in the final reaction mixture. Enzymes were dialyzed into this buffer system containing the appropriate metal concentration (see

Table I: Steady-State Kinetic Parameters[a]

enzyme	metal	pH	K_m^{ATP} (μM)	K_m^{Glu} (mM)	k_{cat} (s^{-1})
$GS_{n=2}$	Mg^{2+}	7.5	150 ± 7	3.3 ± 0.6	33 ± 3
$GS_{n=2}$	Mg^{2+}	6.5	235 ± 5	6.6 ± 1.3	7.7 ± 0.5
$GS_{n=2}$	Mn^{2+}	6.5	1.5 ± 0.3	0.070 ± 0.005	2 ± 0.2
$GS_{n=12}$	Mn^{2+}	6.5	55 ± 3[b]	3.4 ± 0.02[b]	5 ± 1
$GS_{n=12}$	Mg^{2+}	7.5	657 ± 53	6.6 ± 1.0	0.9 ± 0.3

[a] For $GS_{n=2}$, k_{cat} was calculated by using the unadenylylated subunit concentration. All measurements were conducted at 25 °C in buffer containing 100 mM KCl, 50 mM NH_4Cl, and 100 mM Pipes at pH 6.5, and in 100 mM Hepes at pH 7.5. [b] Sager and Villafranca, unpublished results.

below) prior to each reaction. ATP concentrations were determined spectrophotometrically by measuring the absorbance at 259 nm of a 0.1 M solution prepared from the stock solution. For $GS_{n=2}$ with Mn^{2+} as the metal ion, the final reaction mixture contained 8 mM $MnCl_2$, 70 μM unadenylylated subunits, 500 μM ATP, 375 μM glutamate, and 50 mM NH_4Cl at pH 6.5. For $GS_{n=12}$ the final reaction mixture contained 8 mM $MnCl_2$, 39.4 μM adenylylated subunits, 610 μM ATP, 37.5 mM glutamate, and 50 mM NH_4Cl at pH 6.5. For $GS_{n=2}$ with Mg^{2+} as the metal ion, the final reaction mixture contained 25 mM $MgCl_2$, 44 μM unadenylylated subunits, 914 μM ATP, 30 μM glutamate, and 50 mM NH_4Cl at pH 6.5.

Data Analysis. Steady-state kinetic data were analyzed by using the computer program HYPERO (Cleland, 1979) modified for the Macintosh computer. Rapid quench data were fit to eq 2 by a nonlinear least-squares fit, where P_i = (μM) con-

$$P_i/E = A(1 - e^{-\lambda t}) + k_{ss}t \quad (2)$$

centration of radioactive inorganic phosphate, E = concentration of adenylylated or unadenylylated subunits/reaction, A = burst amplitude, k_{ss} = steady-state rate constant, λ = transient phase rate constant, and t = time.

Rapid quench data were also fit by using the computer program KINSIM (Barshop et al., 1983) to simulate the reaction pathway. The program was modified by Johnson to allow the input of data from rapid quench experiments as x,y pairs and to calculate the sum square errors in fitting the data.

Results

Steady-State Kinetics. The steady-state kinetic data obtained for various forms of glutamine synthetase are summarized in Table I. The K_m for either ATP or glutamate was determined by keeping all of the substrates saturating except the variable substrate. With either unadenylylated or adenylylated enzyme, the pH optimum seems to depend on the activating metal ion and is pH 7.5 with Mg^{2+} and pH 6.5 with Mn^{2+} (Ginsburg et al., 1970). When Mn^{2+} is used as the activating metal with $GS_{n=2}$, a sharp decrease in substrate K_m's was observed compared to those measured when Mg^{2+} is the activating metal. The activity observed for $GS_{n=2}$ with Mn^{2+} is not due to activity from the small fraction of adenylylated subunits because the K_m's observed for $GS_{n=12}$ are much different and more importantly much larger. The double-reciprocal plots of the kinetic data for $GS_{n=2}$ with Mn^{2+} exhibited biphasic behavior in the form of apparent substrate activation at high concentrations of either ATP or glutamate. Double-reciprocal plots for completely adenylylated enzyme were not biphasic, which may indicate that at higher substrate concentrations there is some contribution to the observed activity of $GS_{n=2}$ by the small number of adenylylated subunits. $GS_{n=12}$ has a small but measurable amount of activity with Mg^{2+} as the activating metal. Again, the K_m's observed for substrates with $GS_{n=12}$ under these conditions were much larger than those observed for $GS_{n=2}$ with Mg^{2+}, and so the observed activity is not due to the presence of a number of unadenylylated subunits. With either activating metal, the effect of adenylylation is to evaluate the K_m's for both substrates when compared to unadenylylated subunits under identical conditions. Steady-state kinetic determinations were conducted on $GS_{n=2}$ with Mg^{2+} at pH 6.5 as a control to show that the observed decreases in K_m's are indeed due to the metal ion and are not a pH effect.

Table II: Stopped-Flow Kinetic Data for ATP

enzyme	pH	metal	k_1 (μM^{-1} s^{-1})	k_2 (s^{-1})	K_d (μM)	K_d[a] (μM)
$GS_{n=2}$	7.5	Mg^{2+}	0.77 ± 0.01	207 ± 1.6	270	34
$GS_{n=2}$	6.5	Mn^{2+}	4.22 ± 0.08	160 ± 4.8	38	2.5
$GS_{n=12}$	6.5	Mn^{2+}	2.18 ± 0.07	284 ± 6.0	131	18

[a] Measured by fluorometric titration.

Stopped-Flow Kinetic Experiments. The association rate for ATP was determined by observing the time dependence of the increase in fluorescence observed upon mixing various concentrations of ATP with enzyme. The fluorescence trace was fit to a single exponential, and k_{obs} was plotted versus ATP concentration. The experiment was conducted under pseudo-first-order conditions, with the minimum concentration of ATP being a 5-fold excess over enzyme concentration. The observed rate of association may be approximated by $k_{obs} = k_1[ATP] + k_2$, where k_1 is the association rate for ATP and is determined by the slope of the line and k_2 is the dissociation rate and is determined by the intercept. Such plots were linear for all forms of the enzyme examined. Slopes and intercepts were determined by linear regression analysis, and the results are summarized in Table II. The ratio of k_2/k_1 was used to calculate the dissociation constant for the enzyme–ATP complex. The fastest association rate and the tightest binding were observed for $GS_{n=2}$ with Mn^{2+}. Either adenylylation of the enzyme or changing the metal from Mn^{2+} to Mg^{2+} resulted in a slower association rate and larger dissociation constants. These results are consistent with the trend observed for substrate K_m's determined in the steady-state kinetic measurements. Equilibrium measurements of the dissociation constant for ATP with various forms of the enzyme consistently produced smaller K_d's than those measured kinetically; however, the trend remained the same.

Rapid Quench Experiments. Quench flow experiments were conducted with all substrates present at 5–10 times the K_m values measured in the steady-state experiments. Experiments were conducted at 10 °C unless otherwise specified in order to allow more accurate measurement of the burst rates. The time course for the quench flow experiment with $GS_{n=2}$ with Mn^{2+} at pH 6.5 is shown in Figure 1. The concentration of substrates used in this case was chosen to maintain saturating conditions for the unadenylylated subunits but also to minimize any contribution to the observed activity from the adenylylated subunits. The K_m's for ATP and glutamate for $GS_{n=2}$ and $GS_{n=12}$ with Mn^{2+} are different enough to allow a fairly complete separation of the two activities. The time course of the reaction was followed from 5 ms to 4 s with duplicate measurements made at all time points between 5 and 80 ms. The data were fit to eq 2, and the results are summarized in Table III. A burst amplitude of 0.68 was observed. This amplutide is quite similar to that of 0.57 previously observed for $GS_{n=2}$ with Mg^{2+} at pH 7.5.

In contrast to these results, the time course for the quench flow experiment with $GS_{n=12}$ with Mn^{2+} at pH 6.5, shown in Figure 2, reveals a very small burst amplitude. When the data from 5 ms to 2 s were fit to eq 2, the burst amplitude was found

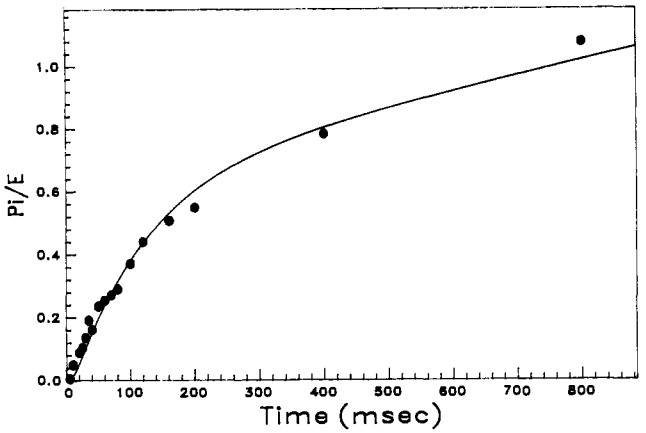

FIGURE 1: Time course of the quench flow kinetic experiment with $GS_{n=2}$ at 10 °C. The final reaction mixture after mixing contained 70 μM unadenylylated subunits, 8 mM $MnCl_2$, 500 μM glutamate, and 50 mM NH_4Cl at pH 6.5. The reaction was followed from 5 ms to 4 s. Data shown are those measured up to 800 ms. The solid dots represent the actual experimental data, and the solid line is the KINSIM fit using the rate constants in Table IV.

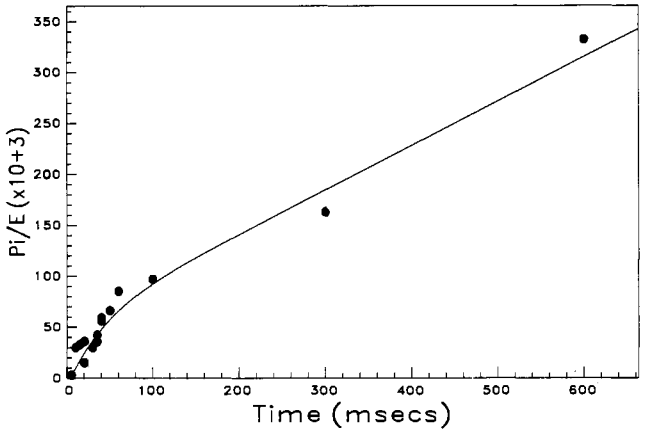

FIGURE 2: Time course of the quench flow kinetic experiment with $GS_{n=12}$ at 10 °C. The final reaction mixture after mixing contained 39.4 μM adenylylated subunits, 8 mM $MnCl_2$, 610 μM ATP, 37.5 mM glutamate, and 50 mM NH_4Cl at pH 6.5. The reaction was followed from 5 ms to 2 s. Data shown are those measured up to 600 ms. The solid dots represent the actual experimental data, and the solid line is the KINSIM fit using the rate constants in Table IV.

Table III: Rapid Quench Kinetic Data

enzyme	k_{burst} (s^{-1})	A	k_{ss} (s^{-1})
$GS_{n=2}$, Mg^{2+}, pH 7.5, 10 °C[a]	88	0.57	4.0
$GS_{n=2}$, Mg^{2+}, pH 6.5, 10 °C	40 ± 20	0.016 ± 0.02	1.20 ± 0.04
$GS_{n=2}$, Mn^{2+}, pH 6.5, 10 °C	6.4 ± 0.4	0.68 ± 0.02	0.47 ± 0.01
$GS_{n=12}$, Mn^{2+}, pH 6.5, 10 °C	24.0 ± 8.8	0.056 ± 0.01	0.43 ± 0.01
$GS_{n=12}$, Mn^{2+}, pH 6.5, 17 °C	40 ± 20	0.056 ± 0.021	1.58 ± 0.04

[a] Previously measured by Meek et al. (1982).

to be 0.056, an order of magnitude smaller than that observed for other forms of the enzyme. To ensure that this result was not due to the temperature at which the experiment was conducted, the experiment was repeated at 17 °C. The burst rate at 17 °S was difficult to measure accurately by fitting the data to eq 2; however, accurate values for the burst amplitude could be obtained, and this amplitude was found to be identical with that measured at 10 °C. As a control, a quench flow experiment was carried out with $GS_{n=2}$ with Mg^{2+} at pH 6.5 so that the effect of pH could be determined. Again, the burst rate was too fast to measure accurately, but accurate values for the burst amplitude and the steady-state rate could be obtained by fitting the data to eq 2. Rapid quench experiments could not be conducted on $GS_{n=12}$ with Mg^{2+} as the activating metal because the K_m for ATP for this form of the enzyme was too large for the experiment to be conducted under saturating conditions. The data are summarized in Table III.

Scheme I

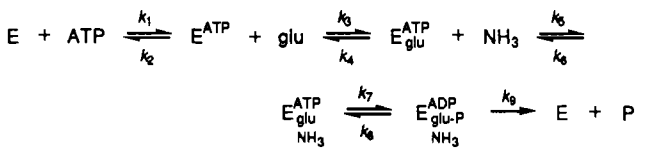

Table IV: Calculated Kinetic Constants from Rapid Quench Data

enzyme	k_7 (s^{-1})	k_8 (s^{-1})	k_9 (s^{-1})	k_7/k_8
$GS_{n=2}$, Mg^{2+} pH 7.5, 10 °C[a]	54	28	9	1.9
$GS_{n=2}$, Mg^{2+}, pH 6.5, 10 °C	8.0	25	5.7	0.32
$GS_{n=2}$, Mn^{2+}, pH 6.5, 10 °C	4.8	1.0	0.62	4.8
$GS_{n=12}$, Mn^{2+}, pH 6.5, 10 °C	1.8	16.4	5.8	0.11
$GS_{n=12}$, Mn^{2+}, pH 6.5, 17 °C	3.7	19.1	17.3	0.19

[a] Previously measured by Meek et al. (1982).

The results of the rapid quench experiments may be related to rate constants in the biosynthetic reaction for glutamine synthetase initially by the analysis utilized by Meek et al. (1982). The rate constants for individual steps in the biosynthetic reaction can be represented as shown in Scheme I. In this scheme k_7 represents the phosphoryl-transfer step and k_9 includes the ammonolysis step as well as product release steps. Since the substrate concentrations were saturating in each experiment and therefore the association rates for substrates are presumably fast, eq 3–5 may be used to relate k_7, k_8, and k_9 to the experimental values obtained from rapid quench experiments.

$$k_{ss} = \frac{k_7 k_9}{k_7 + k_8 + k_9} \tag{3}$$

$$A = \frac{k_7(k_7 + k_8)}{(k_7 + k_8 + k_9)^2} \tag{4}$$

$$\lambda = k_7 + k_8 + k_9 \tag{5}$$

The results of these calculations are summarized in Table IV. In cases where large errors in the measured burst rate made accurate rate constant calculations infeasible using eq 3–5, kinetic constants were determined by simulating the mechanism shown in Scheme I according to the KINSIM program. The simulation results could be overlaid on the experimental data so that the best fit could be determined. For initial data fits, the association rates for all substrates were assumed to be fast, and values for k_7, k_8, and k_9 were then obtained. Where more accurate values for the burst rate were obtained from fitting the experimental data to eq 2, KINSIM simulations were found to be in complete agreement with the rate constants calculated from eq 3–5. KINSIM simulations could therefore be used with confidence to obtain kinetic constants.

DISCUSSION

From steady-state kinetic measurements it has become clear that regardless of the metal ion type, adenylylation significantly increases the K_m's for both ATP and glutamate (Table I). This result is consistent with the observation that the K_d for Mn^{2+} as measured by EPR titration experiments increases by an order of magnitude when low adenylylation enzyme is compared to high adenylylation state enzyme (Villafranca et al., 1976; Villafranca & Wedler, 1974). In vivo, therefore, adenylylation functions to turn glutamine synthetase activity off by resulting in poorer metal binding and by elevating the K_m's of substrates well above their physiological concentrations.

The effect of metal ion type can be clearly seen by comparing kinetic data on enzyme of the same adenylylation state, either low or high with either metal ion. In both cases, changing the metal ion from Mn^{2+} to Mg^{2+} results in large increases in the K_m's observed for both ATP and glutamate (Table I). This result mirrors other kinetic observations which have indicated that Mg^{2+} binds approximately 200-fold less tightly than Mn^{2+} (Denton & Ginsburg, 1970). Recent free energy calculations on Ca-binding proteins have indicated that differences in solvation energies may be responsible for these proteins binding Ca^{2+} preferentially over Mg^{2+} (Sussman & Weinstein, 1989). Mg^{2+}, with its smaller ionic radius of 0.78, is preferentially solvated compared to the large Ca^{2+} ion which has an ionic radius of 1.06. Mn^{2+} has an ionic radius of 0.91 and therefore resembles Ca^{2+} in solvation preference. The size differential between Mn^{2+} and Mg^{2+} may explain the greater preference exhibited by Mn^{2+} for binding to the hydrophobic active site of glutamine synthetase. The K_d's measured for ATP from fluorescence measurements show the same trend of weaker binding of ATP when comparing Mn^{2+} to Mg^{2+} and low adenylylation state enzyme with high adenylylation state enzyme (Table II). Both on-rates and off-rates appear to be affected to some extent by metal ion type and adenylylation. Additionally, the dissociation constants calculated from the kinetic data are consistently higher than those determined by an equilibrium method (Table II), suggesting that there is a rapid prior equilibrium step for ATP binding which should also appear in Scheme I. Further experiments are planned to address this step in the mechanism.

The kinetic constants derived from rapid quench experiments for different forms of the enzyme are summarized in Table IV. Changing the activating metal ion from Mg^{2+} to Mn^{2+} with low adenylylation state enzyme appears to make all of the chemical steps slower; however, the rate-limiting step is still product release in both cases. The internal equilibrium constant for phosphoryl transfer is slightly more than doubled, and this reflects the larger rate reduction observed for k_8, the reverse phosphoryl-transfer step, when Mn^{2+} is substituted for Mg^{2+}. The rate reduction in all of the steps observed with the Mn^{2+} form of the low adenylylation state enzyme may reflect the tighter binding of Mn^{2+} and the correspondingly tighter binding of substrates compared to the Mg^{2+} form of the enzyme. The overly effective stabilization of bound ground-state substrates and/or products by the enzyme may well be responsible for the decreased catalytic flux of the Mn^{2+} form of the unadenylylated enzyme.

Since the pH optimum for the Mn^{2+} form of the enzyme is different than that for the Mg^{2+} form of the enzyme, the effect of pH on the energetics of the reaction was investigated. When the pH is changed from 7.5 to 6.5 with Mg^{2+} and low adenylylation state enzyme, the rate-limiting step is still found to be product release; however, this pH change has a much larger effect on k_7, the forward phosphoryl-transfer step, than k_8. The observed decrease in k_7 is probably not surprising as the chemistry is now becoming more rate limiting farther away from the pH optimum for the enzyme. However, there is almost no change in k_8, indicating that the Mn^{2+} ion itself and not the pH of the reaction is responsible for the large reduction in k_8. The large decrease in the internal equilibrium constant for phosphoryl transfer in this case is due almost entirely to the decrease in k_7.

In contrast to the results with low adenylylation state enzyme and either metal ion or pH, rapid quench experiments with the adenylylated enzyme showed only a very small burst amplitude. Subsequent calculation of rate constants from these

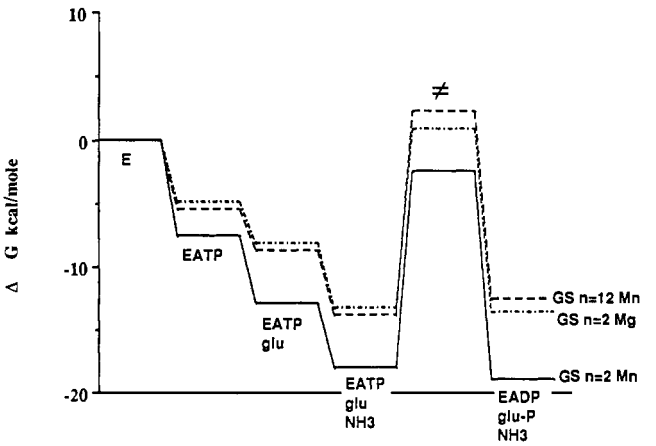

FIGURE 3: Free energy diagram for three different forms of GS. The profile was constructed by using the K_m values for each substrate (Table I), and the rate constants were calculated from rapid quench experiments (Table IV). A standard state of 1 M was used.

results showed that product release is no longer rate limiting for this enzyme but that the rate-limiting step is now phosphoryl transfer. This experiment was repeated at 17 °C, and the rate-limiting step remained the same, indicating that this result is not temperature dependent.

The free energy diagram shown in Figure 3 for the different forms of the enzyme was constructed by using the rate constants calculated from the rapid quench experiments. The low adenylylation state enzyme with Mn^{2+} shows significant stabilization of intermediates throughout compared to the other forms of the enzyme consist with its tighter binding of substrates. $GS_{n=2}$ with Mg^{2+} and $GS_{n=12}$ with Mn^{2+} initially show similar stabilization of bound substrates as expected from the similar K_m's for these two enzymes; however, $GS_{n=12}$ does not appear to stabilze the transition state for phosphoryl transfer as well as the other forms of the enzyme. $GS_{n=12}$ also does not stabilize the γ-glutamyl phosphate intermediate as well as either of the other forms of the enzyme and in addition does not stabilize this intermediate better than the ternary complex as evidenced by the large rate constant for the reverse phosphoryl-transfer reaction. These results strongly suggest a significant influence on the geometry and/or the electronics of the active site due to the covalent adenylylation modification consistent with previous UV and calorimetric measurements (Ginsburg, 1972; Gorman & Ginsburg, 1982).

Free Energy Profile for Phosphoryl Transfer by Adenylylated and Unadenylylated Glutamine Synthetase. The Gibbs free energy profiles for substrate binding and the formation of the γ-glutamyl phosphate intermediate by low adenylylation state and adenylylated GS with either Mn^{2+} or Mg^{2+} as the activating metal ion are shown in Figure 3. These profiles were constructed by using the K_m values for each substrate (Table I) and the rate constants calculated from rapid quench experiments (Table IV). A standard state of 1 M was assumed for all substrates (Wells & Fersht, 1986).

The results reflect the sensitive interplay between how well an enzyme can bind ground-state substrates, stabilize intermediates, and be an effective catalyst. The low adenylylation state enzyme with Mn^{2+} shows a significantly greater stabilization of substrates and intermediate compared to the other forms of the enzyme. While the enzyme has a favorable internal equilibrium constant for phosphoryl transfer in the forward direction of 5, this increased stabilization results in slower rate constants for both forward and reverse phosphoryl transfer (Table IV) and a greatly reduced k_{cat} compared to the Mg^{2+} form of the enzyme. On going from low adenyl-

ylation state to high adenylylation state enzyme with Mn^{2+}, k_{cat} is increased slightly probably due to looser binding of substrates; however, catalysis is not completely optimized due to poor stabilization of the transition state for phosphoryl transfer and binding of the γ-glutamyl phosphate intermediate. $GS_{n=12}$ is unable to sufficiently stabilize the γ-glutamyl phosphate intermediate compared to the ternary complex as indicated by an internal equilibrium constant of 0.2 for phosphoryl transfer, and so a substantial amount of catalytic throughput is lost due to the increased value of the rate constant for the reverse phosphoryl transfer. Low adenylylation state GS with Mg^{2+} stabilizes bound substrates in a similar fashion to $GS_{n=12}$ with Mn^{2+}. However, this form of the enzyme also has the ability to stabilize both the transition state for phosphoryl transfer (compared to $GS_{n=12}$) and the γ-glutamyl phosphate intermediate relative to the ternary complex. This latter point is indicated by an internal equilibrium constant for phosphoryl transfer of 2. Low adenylylation state glutamine synthetase with Mg^{2+} shows the fastest rate constants for phosphoryl transfer because it does not overly stabilize bound ground-state substrates as does the Mn^{2+} form of the enzyme. In addition, low adenylylation state enzyme can still sufficiently stabilize the important chemical intermediates, which the adenylylated enzyme cannot. These factors combined give maximum catalytic flux and make low adenylylation state glutamine synthetase with Mg^{2+} the optimized form of the enzyme for catalysis.

References

Almassy, R. J., Janson, C. A., Hamlin, R., Xuong, N.-H., & Eisenberg, D. (1986) *Nature 323*, 304.

Backman, K., Chen, Y.-M., & Magasanik, B. (1981) *Proc. Natl. Acad. Sci. U.S.A. 78*, 3743–3747.

Barshop, B. A., Wrenn, R. F., & Frieden, C. (1983) *Anal. Biochem. 130*, 134.

Cleland, W. W. (1979) *Methods Enzymol. 63*, 103.

Denton, M. D., & Ginsburg, A. (1970) *Biochemistry 9*, 617.

Ginsburg, A. (1972) *Adv. Protein Chem. 26*, 1–79.

Ginsburg, A., & Stadtman, E. R. (1973) in *The Enzymes of Glutamine Metabolism* (Prusiner, S., & Stadtman, E. R., Eds.) pp 9–44, Academic Press, New York.

Ginsburg, A., Yeh, J., Hennig, S. B., & Denton, M. D. (1970) *Biochemistry 9*, 633.

Gorman, E. G., & Ginsburg, A. (1982) *J. Biol. Chem. 257*, 8244–8252.

Hennig, S. B., & Ginsburg, A. (1971) *Arch. Biochem. 144*, 611.

Holzer, H. (1969) *Adv. Enzymol. Relat. Areas Mol. Biol. 32*, 297–326.

Johnson, K. A. (1986) *Methods Enzymol. 134*, 677.

Lewis, D. A., & Villafranca, J. J. (1989) *Biochemistry 28*, 8454.

Magasanik, B., & Reitzer, L. J. (1987) in *Escherichia coli & Salmonella Typhimurium—Cellular and Molecular Biology* (Neidhardt, F. C., Ed.) Vol. 1, pp 302–320, American Society for Molecular Biology, Washington, D.C.

Meek, T. D., Johnson, K. A., & Villafranca, J. J. (1982) *Biochemistry 21*, 2158.

Miller, R. E., Shelton, E., & Stadtman, E. R. (1974) *Arch. Biochem. Biophys. 163*, 155.

Morrison, J. F. (1979) *Methods Enzymol. 63*, 257.

Rhee, S. G., Chock, P. B., & Stadtman, E. R. (1985) *Methods Enzymol. 113*, 213.

Roseman, J. E., & Levine, R. L. (1987) *J. Biol. Chem. 262*, 2101.

Shapiro, B. M., Kingdon, H. S., & Stadtman, E. R. (1967) *Proc. Natl. Acad. Sci. U.S.A. 58*, 642.

Stadtman, E. R., & Ginsburg, A. (1974) in *The Enzymes* (Boyer, P. D., Ed.) Vol. 3, p 755, Academic Press, New York.

Stadtman, E. R., Smyrniotis, P. Z., Davis, J. N., & Wittenberger, M. E. (1979) *Anal. Biochem. 85*, 275.

Stadtman, E. R., Mura, E., Chock, P. B., & Rhee, S. G. (1980) in *Glutamine: Metabolism, Enzymology & Regulation* (Mora, J., & Palacios, R., Eds.) pp 41–59, Academic Press, New York.

Sussman, F., & Weinstein, H. (1989) *Proc. Natl. Acad. Sci. U.S.A. 86*, 7880–7884.

Villafranca, J. J., & Wedler, F. C. (1974) *Biochemistry 13*, 3286.

Villafranca, J. J., Ash, D. E., & Wedler, F. C. (1976) *Biochemistry 15*, 536–543.

Wells, T. N. C., & Fersht, A. R. (1986) *Biochemistry 25*, 1881–1886.

Yamashita, M. M., Almassy, R. J., Janson, C. A., Cascio, D., & Eisenberg, D. (1989) *J. Biol. Chem. 264*, 17681.